Characteristics of Dielectrically Loaded Ladder Lines for Traveling-Wave Masers and Other Applications

GEORGE I. HADDAD, MEMBER, IEEE

Abstract—The characteristics of ladder lines are investigated in detail and the effects of the various dimensions of the ladder line and the enclosing structure on the ω-β characteristic are presented. The effects of a dielectric material placed at different positions in the structure on the characteristics are also examined in detail. Dielectric materials selected for investigation have relative dielectric constants of 9, 100, and 256, characteristic of ruby and rutile, which have been shown to be good maser materials.

It is shown that a nonpropagating easitron circuit may be made to propagate by loading it with a dielectric material, in which case the ridge in a Karp-type slow-wave structure may be eliminated. This results in a simple traveling-wave maser structure.

The input impedance to the ladder-line structure and the structure ohmic loss have been evaluated and are presented in the figures. This information is useful in designing transducers to couple the power into and out of the structure, and gives an estimate of the expected ohmic loss in the structure.

Introduction

IT IS WELL known that the gain in a traveling-wave maser [1] is directly proportional to the slowing factor of the structure (i.e., the ratio of the velocity of light to the group velocity) and is inversely proportional to the magnetic Q of the maser material. The magnetic Q of the maser material depends on the RF field configuration in the structure and also on the filling factor. It is thus very desirable in the design of traveling-wave masers that one be able to predict the pertinent characteristics of the slow-wave structure without having to resort to detailed measurements which can be very time consuming. Especially since the dielectric maser material is an integral part of the amplifier, it is very desirable to determine the effect of the dielectric material on the characteristics of the slow-wave structure. In order to achieve this, a space-harmonic analysis, which was originated by Fletcher [2] in connection with his work on the interdigital line circuit, has been employed to study the effect of different dielectric materials on the characteristics of ladder-line slow-wave structures [3]. This analysis yields useful information on the ω-β characteristic, the input impedance, "fold-over" modes [4] which lead to unstable operation of the maser, the RF field configuration for determining the magnetic Q, and the ohmic loss in the structure.

The effect on the characteristics of the ladder-line structure of materials with relative dielectric constants of 9 (ruby), 100, and 256[1] (rutile) have been considered and the results appear in great detail in Haddad [5]. Some typical results are presented here. Several of the results presented here should prove useful in the design of traveling-wave masers utilizing other structures such as the comb [1], [6], meander-line [7], and waveguide structures.

This structure has been widely used in traveling-wave amplifiers and backward-wave oscillators [3] in the millimeter-wave region and also in traveling-wave masers [8]–[10]. It is believed that the results of this analysis lead to improved design criteria for such structures.

Space Harmonic Analysis

A general cross-sectional view and pertinent dimensions of a dielectrically loaded ladder-line or Karp-type slow-wave structure are shown in Fig. 1. This analysis is applicable to any form of a dielectrically loaded ladder line. The different forms are the easitron, the single ridge, the double ridge, the single trough, and the double trough. These different forms are obtained by merely changing the a dimensions relative to the b dimensions [11].

Butcher [11] employed a field theory analysis to study the dispersion characteristics of empty[2] ladder-line slow-wave structures. He neglected the thickness of the tapes and assumed E_y and H_y to be negligible in the plane of the ladder, which implies that a TEM wave propagates along the tapes. The method of analysis employed here was first employed by Fletcher [2] in his study of the interdigital line and later by Walling [12] in his study of other slow-wave structures. This analysis essentially consists of building up the complete solution in terms of a series of TEM waves which are assumed to propagate along the tapes of the structure with the velocity of light. This assumption is not quite true due to the presence of the ridge in the structure and will not be quite true in regions where a dielectric material is present. This is because TEM propagation, strictly speaking, is not possible when the space is made inhomogeneous. It is believed, however, that this method, even though approximate, will lead to generally satisfactory results and will approximately predict the effect of the tape thickness and the dielectric material on the characteristics of the structure. Another approximation which

Manuscript received October 22, 1964; revised November 15, 1965. The work reported herein was supported by the Electronic Technology Division, Air Force Avionics Laboratory, under Contract AF-33(615)-1553.

The author is with the Department of Electrical Engineering, The University of Michigan, Ann Arbor, Mich.

[1] The results for $\epsilon_r = 256$ are similar to those of $\epsilon_{r2} = 100$ and are not presented here due to lack of space.

[2] An empty structure is one which contains no dielectric material.

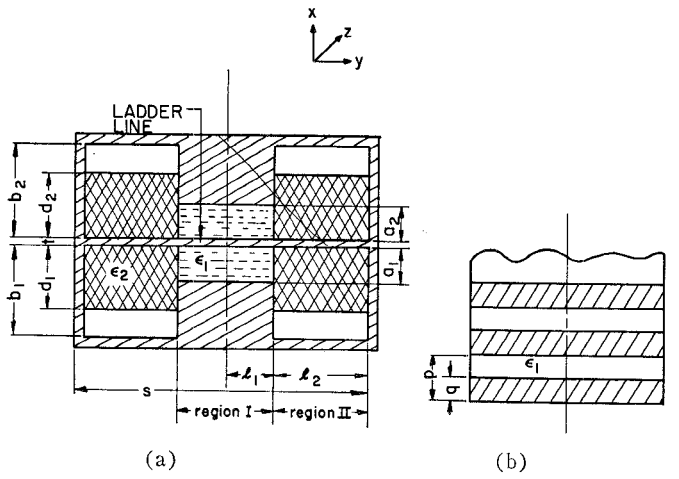

Fig. 1. Dielectrically loaded ladder-line slow-wave structure. (a) Structure cross section. (b) Ladder line.

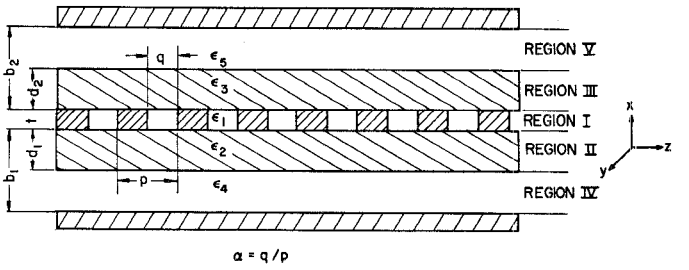

Fig. 2. Cross section of a dielectrically loaded ladder line.

is used in this analysis is the assumption that the electric field (E_z) is constant between the ladder tapes. Ash and Studd [13] have compared the dispersion characteristics of a zero-thickness ladder line using this approximation with a rigorous solution obtained by Butcher [14] and found that the discrepancy is fairly small. The experimental results on an X-band traveling-wave maser [10] using a ruby-loaded ladder line are in good agreement with the results obtained from this theory.

Since the ladder-line structure is symmetrical, only one half of it need be considered. This is divided into the two regions as shown in Fig. 1. The other dimensions of the structure are shown in Fig. 2. The geometry of the structure is repeated at each conductor and, thus, only one space harmonic is required to satisfy the field distribution. Following Fletcher [2] and Walling [12], the dispersion equations for the symmetric and antisymmetric modes may be expressed as follows:

1) symmetric mode

$$\tan k_1 l_1 \tan k_2 l_2 = Y_2(\theta)/Y_1(\theta) \tag{1}$$

2) antisymmetric mode

$$\tan k_2 l_2 \cot k_1 l_1 = -Y_2(\theta)/Y_1(\theta) \tag{2}$$

where

k_1 and k_2 = the propagation constants in Regions I and II, respectively,

$Y_1(\theta)$, $Y_2(\theta)$ = the Fletcher admittance functions of Regions I and II, respectively, and

θ = phase shift per period.

Equations (1) and (2) may now be employed to determine the dispersion characteristics of the structure. In order to accomplish this, however, $Y_2(\theta)$, $Y_1(\theta)$, k_2, and k_1 must be determined. The question arises as to what value of k must be employed in a region containing a dielectric material. The approach employed here is to define an effective dielectric constant for the region under consideration and to employ this to determine the effective k and the admittance for the region.

The effective dielectric constant is defined in a manner similar to that employed by Chen [15] in a recent analysis of a dielectrically loaded comb structure. Namely, it is assumed that a dielectric material with a relative dielectric constant ϵ_{eff} fills the entire region, and the charge induced on the tapes is assumed to be equal to the charge induced when the region is partially filled with a dielectric.

The method for obtaining an expression for ϵ_{eff} is discussed in detail in Haddad [5] and Chen [15] and will not be included here.

Based on the "Equal-Charge Approximation," the effective dielectric constant may be expressed as

$$\epsilon_{\text{eff}} = \frac{4\epsilon_{r1}\dfrac{t}{q}\sin^2\theta/2 + 2(1-\alpha)\sin\theta/2\left[\epsilon_{r3}S_2(b_2, d_2, \alpha) + \epsilon_{r2}S_2(b_1, d_1, \alpha)\right]}{4\dfrac{t}{q}\sin^2\theta/2 + 2(1-\alpha)\sin\theta/2\left[S_1(b_1, 0, \alpha) + S_1(b_2, 0, \alpha)\right]}, \tag{3}$$

where

$$S_2(b, d, \alpha) = \sum_{m=-\infty}^{\infty}(-1)^m \tanh\beta_m d \cdot \left[\frac{1 + \epsilon_5/\epsilon_3 \coth\beta_m d \coth\beta_m(b-d)}{1 + \epsilon_5/\epsilon_3 \coth\beta_m(b-d)\tanh\beta_m d}\right] \cdot \left[\frac{\sin\left(\frac{1-\alpha}{2}\right)(\theta + 2\pi m)\sin\frac{\alpha}{2}(\theta + 2\pi m)}{\left(\frac{1-\alpha}{2}\right)(\theta + 2\pi m)\frac{\alpha}{2}(\theta + 2\pi m)}\right] \tag{4}$$

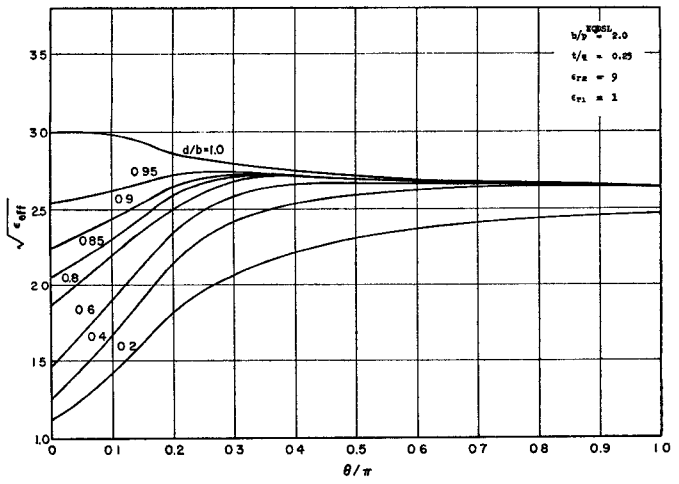

Fig. 3.

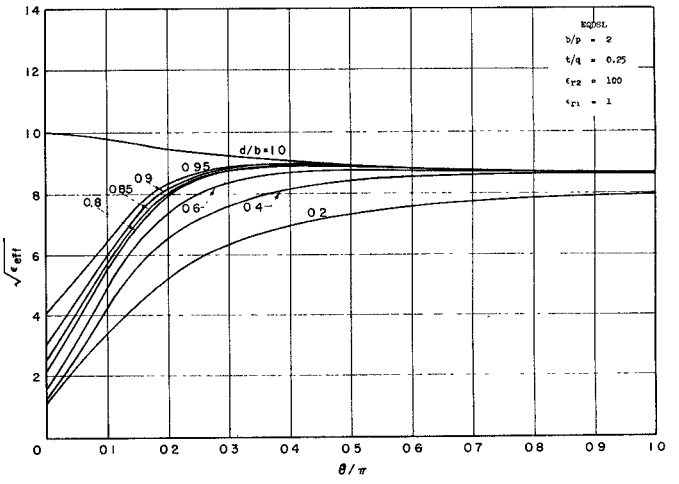

Fig. 4.

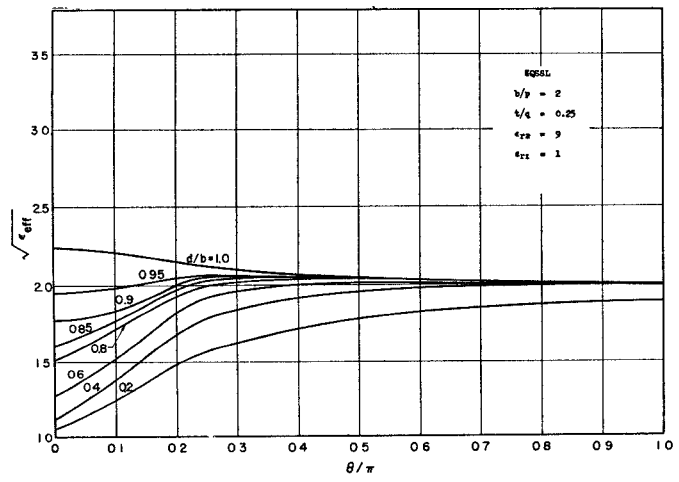

Fig. 5.

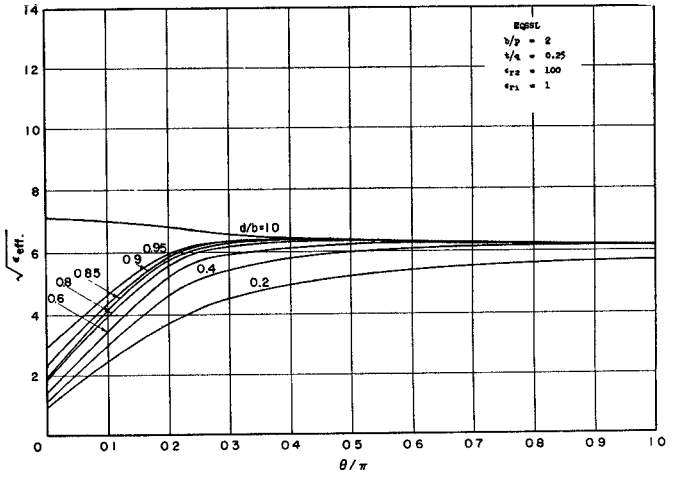

Fig. 6.

Figs. 3–6. $\sqrt{\epsilon_{eff}}$ vs. θ/π.

and

$$S_1(b, 0, \alpha) = \sum_{m=-\infty}^{\infty} (-1)^m \coth \beta_m d \cdot \left[\frac{\sin\left(\frac{1-\alpha}{2}\right)(\theta + 2\pi m) \sin\frac{\alpha}{2}(\theta + 2\pi m)}{\left(\frac{1-\alpha}{2}\right)(\theta + 2\pi m)\frac{\alpha}{2}(\theta + 2\pi m)} \right]. \quad (5)$$

The following functions are now defined:

$$f_2 \triangleq \frac{S_1(b, 0, 0.5)}{2} \sin \theta/2 \quad (6)$$

and

$$f_3 \triangleq \frac{S_2(b, d, 0.5)}{2} \sin \theta/2. \quad (7)$$

f_2 and f_3 are plotted by Haddad [5] as a function of θ/π for several values of d/b, d/p, and $\epsilon_r = \epsilon_3/\epsilon_5$.

A. Double-Side Loading in a Symmetric Structure

It is assumed in this case that the structure is symmetric about the ladder line and that a dielectric material is symmetrically placed above and below the ladder (i.e., $d_1 = d_2$, $b_1 = b_2$, $\epsilon_2 = \epsilon_3$, $\epsilon_5 = \epsilon_4 = \epsilon_0$). ϵ_{eff} may then be expressed by

$$\epsilon_{eff} = \frac{\epsilon_{r1}\frac{t}{q}\sin^2\theta/2 + \epsilon_{r2}f_3}{\frac{t}{q}\sin^2\theta/2 + f_2}. \quad (8)$$

The $\sqrt{\epsilon_{eff}}$ for this case is plotted in Haddad [5] for several different values of the parameters which appear in the equation. Typical results are shown in Figs. 3 and 4 for a particular set of parameters.[3]

B. Single-Side Loading in a Symmetric Structure

Here it is assumed that the structure is loaded on one side of the ladder line while the other side is empty. The

[3] The symbols EQDSL which appear on the figures refer to "Equal-Charge Approximation, Double-Side Loading."

structure is also assumed to be symmetric (i.e., $d_2=0$, $b_1=b_2$, $\epsilon_4=\epsilon_5=\epsilon_3=\epsilon_1$). ϵ_{eff} may then be expressed as

$$\epsilon_{eff}=\frac{\frac{t}{q}\epsilon_{r1}\sin^2\theta/2+\frac{1}{2}[\epsilon_{r1}f_2+\epsilon_{r2}f_3]}{\frac{t}{q}\sin^2\theta/2+f_2}. \tag{9}$$

The $\sqrt{\epsilon_{eff}}$ for this case is also plotted in Haddad [5] for several values of the parameters. Typical cases are shown in Figs. 5 and 6 for a particular set of parameters.[4]

Dispersion Characteristics

The dispersion equations for the symmetric and antisymmetric modes were given in the second section. The symmetric mode is of most interest and is investigated in this section.

It was shown in the second section that the dispersion equation for the symmetric mode may be expressed as[5]

$$\tan k_1l_1\tan k_2l_2=Y_2(\theta)/Y_1(\theta), \tag{10}$$

where the subscripts 1 and 2 refer to Regions I and II, respectively. $Y(\theta)$ is related to $Y_0(\theta)$ as

$$Y(\theta)=\sqrt{\epsilon_{eff}}\,Y_0(\theta), \tag{11}$$

where $Y_0(\theta)=$ the admittance per tape of the empty structure, and k is related to k_0 as

$$k=\sqrt{\epsilon_{eff}}\,k_0, \tag{12}$$

where k_0 is the free space propagation constant.

In traveling-wave maser applications, the active maser material is placed in a region of high magnetic field intensity. This corresponds to Region II of Fig. 1 in this case. The dispersion characteristics are then investigated in detail for such a case, where it is assumed that Region I is empty ($\epsilon_1=\epsilon_0$). In certain applications, such as low-frequency traveling-wave masers, it might be desirable also to load the structure in Region I in order to reduce its size [9].

If it is assumed that the effective dielectric constant in Region I is unity (unloaded), and if a normalized parameter x is defined,

$$x\triangleq\frac{s}{\lambda_0}, \tag{13}$$

where

$s=$ the total width of the structure

and

$\lambda_0=$ free space wavelength,

then (10) may be written in the following form:

$$\tan x(\delta_1\pi/2)\tan\sqrt{\epsilon_{2eff}}\,x(\delta_2\pi/2)=\sqrt{\epsilon_{2eff}}\,\frac{Y_{02}(\theta)}{Y_{01}(\theta)}, \tag{14}$$

where

$$\delta_1=4(l_1/s)$$

and

$$\delta_2=4(l_2/s).$$

Equation (14) may be written in terms of the function f_2, which was defined previously as follows ($\alpha=0.5$):

$$\tan x(\delta_1\pi/2)\tan\sqrt{\epsilon_{2eff}}\,x(\delta_2\pi/2)=\sqrt{\epsilon_{2eff}}\cdot\frac{\frac{t}{q}\sin^2\theta/2+\frac{1}{2}[f_2(b_2,0,0.5)+f_2(b_1,0,0.5)]}{\frac{t}{q}\sin^2\theta/2+\frac{1}{2}[f_2(a_2,0,0.5)+f_2(a_1,0,0.5)]}. \tag{15}$$

In all the cases considered, the empty structure is assumed to be symmetric with respect to the ladder (i.e., $a_1=a_2$, $b_1=b_2$) so that (15) becomes

$$\tan x(\delta_1\pi/2)\tan\sqrt{\epsilon_{2eff}}\,x(\delta_2\pi/2)=\sqrt{\epsilon_{2eff}}\,\frac{\frac{t}{q}\sin^2\theta/2+f_2(b,0,0.5)}{\frac{t}{q}\sin^2\theta/2+f_2(a,0,0.5)}. \tag{16}$$

Equation (16) may now be employed to compute the ω-β characteristic of the structure since all the quantities appearing in that equation are now known. This has been done in detail in Haddad [5]. There, the ω-β characteristic for several different values of the parameters appearing in (16) has been calculated and plotted in the form of universal graphs. A typical set of characteristics is shown and discussed in the following.

A. ω-β Characteristics

Equation (16) was employed to determine the effects of different dielectric materials and dimensions of the structure on the ω-β characteristics. A typical set of results are shown in Figs. 7 through 14. In these figures, the normalized parameter x is plotted as a function of θ/π. The slowing factor S which appears in the traveling-wave maser-gain equation [1] may be expressed as

$$S=\left(\frac{s}{2p}\right)\frac{d\theta/\pi}{dx}. \tag{17}$$

$(d\theta/\pi)/dx$ may be obtained from the figures, s is determined by the signal frequency, and p, the pitch, may be chosen to give the desired slowing factor.

Since x vs. θ/π is plotted for several different parameters and configurations in Figs. 7 through 14, these figures are divided into several categories and the effect of the different parameters in each category is discussed.

[4] The symbols EQSSL which appear on the figures refer to "Equal-Charge Approximation, Single-Side Loading."

[5] The reader should refer to Fig. 1 for identification of the dimensions and regions employed in this discussion.

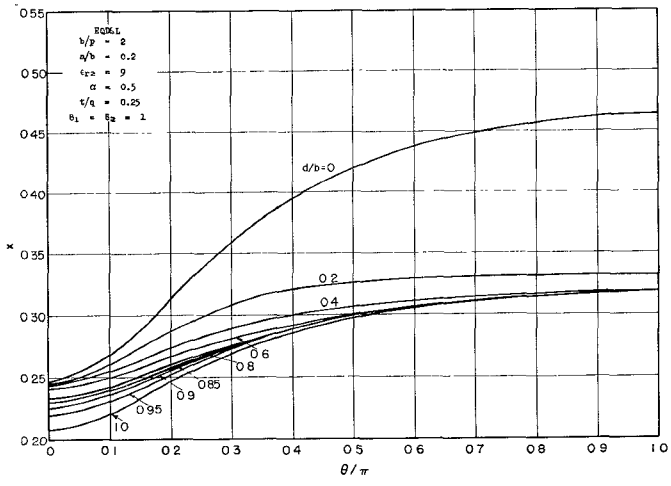

Fig. 7.

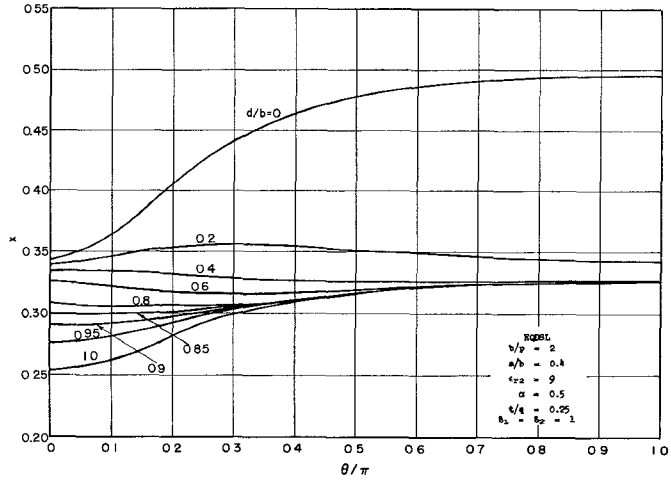

Fig. 8.

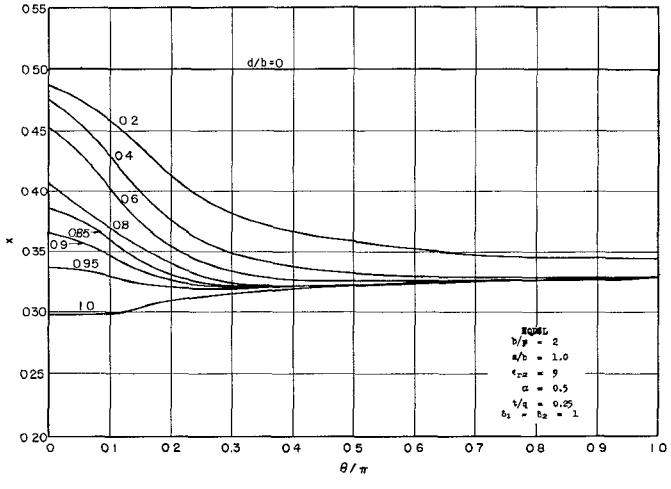

Fig. 9.

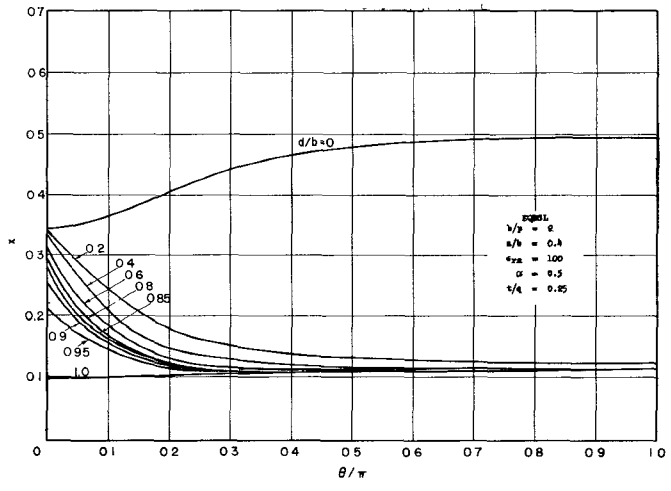

Fig. 10.

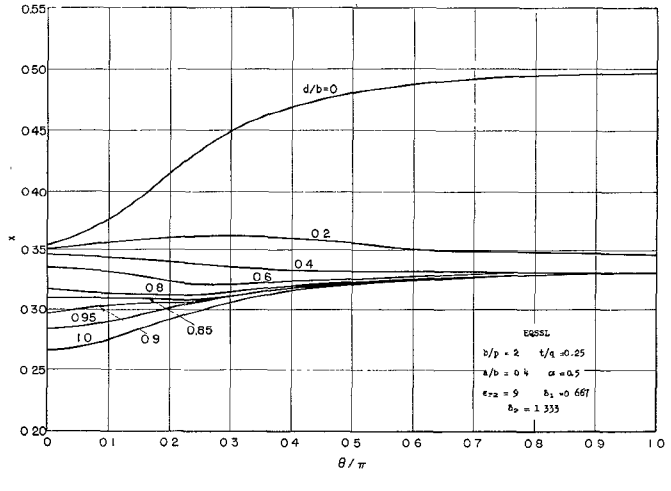

Fig. 11.

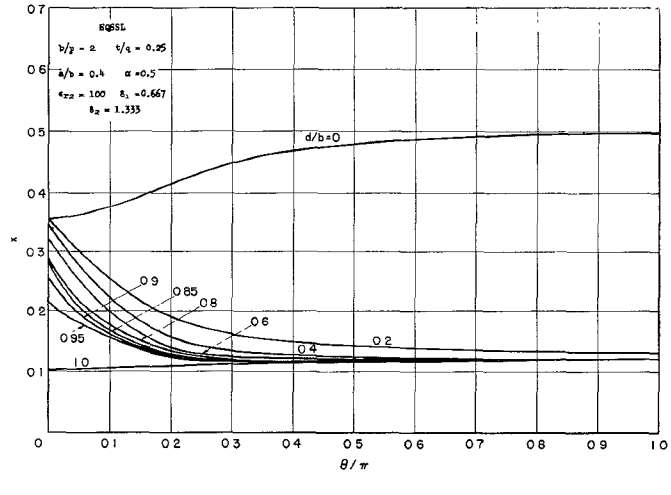

Fig. 12.

Figs. 7–14. x vs. θ/π. (*cont'd. next page*)

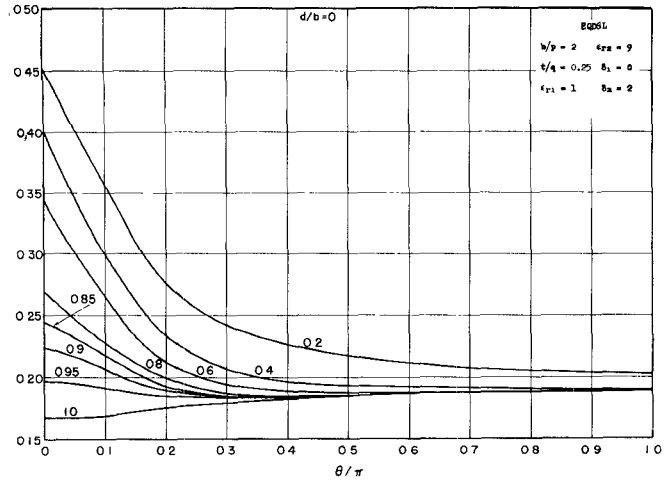

Fig. 13.

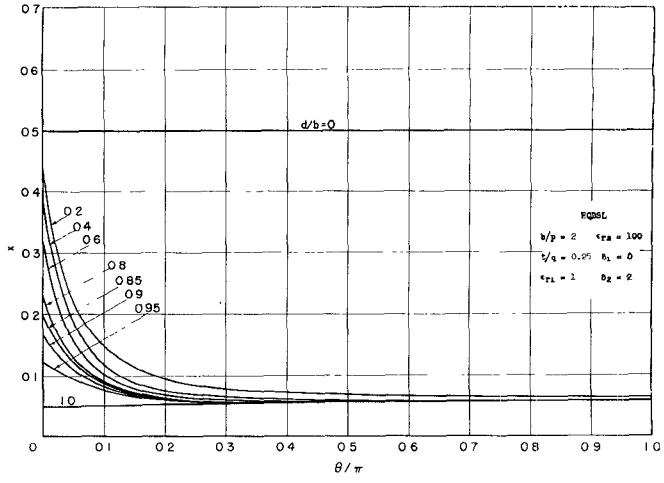

Fig. 14.

All the results given here apply to $\alpha = 0.5$, $\epsilon_1 = \epsilon_0$, $d_1 = d_2$, and $b_1 = b_2$.[6]

Double-side loading refers to the case in which the dielectric material is placed on both sides of the ridge above and below the ladder line. Single-side loading refers to the case in which the dielectric material is placed on both sides of the ridge *either* above *or* below the ladder line.

1. Double-Side Loading ($\delta_1 = \delta_2 = 1$, $t/q = 0.25$, $\epsilon_1 = \epsilon_0$): This case was investigated for three different values of ϵ_{r2}, namely 9 (ruby), 100, and 256 (rutile). A typical set of characteristics for $\epsilon_{r2} = 9$ is shown in Fig. 8. The effect of the dielectric material on the ω-β characteristic is clearly demonstrated in Fig. 8. It is seen, for example, that for a certain set of parameters of the structure (i.e., for a given a/b, δ_1, δ_2, and t/q), varying d/b has a diverse effect on the ω-β characteristic. It is seen that when the structure is filled with a dielectric ($d/b = 1$), both the upper and lower cutoff frequencies are decreased and the total passband is generally decreased. Decreasing d/b raises the lower cutoff frequency while keeping the upper cutoff frequency approximately the same and thus results in a decrease of the total passband and, of course, in a higher slowing factor.

This procedure was first employed at the Bell Telephone Laboratories [1] to obtain high slowing factors in the comb structure. It was also employed in a Karp-type structure [8], [10]. When d/b is decreased further, a foldover mode usually results, since the phase constant becomes a double-valued function of frequency and a backward and forward wave exist at the same frequency. This situation must be avoided in a traveling-wave maser since it leads to unstable operation [4]. When d/b is decreased even further, a backward-wave mode results. The ratio of d/b at which a foldover or backward-wave mode sets in depends on the dielectric constant of the material and the ratio of a/b. It may be seen, for example in Fig. 7, that for $a/b = 0.2$ (ridge close to ladder), even for very small values of d/b, a forward mode still exists. However, for $a/b = 1$ (Fig. 9, no ridge), a backward mode results even for $d/b = 0.95$.

By reference to Fig. 9, which applies to the case where no ridge is present ($a/b = 1.0$), it can be seen that for $d/b = 0$ (empty structure) the passband is zero (easitron circuit); however, a finite passband results when the structure is loaded with a dielectric material. If the dielectric material fills the entire space between the ladder line and the enclosing plates, a forward wave results with a narrow passband. Any small decrease in d/b will result in a foldover mode or a backward wave and, thus, the tolerances in the dimensions of the material become very critical in this case.

As is well known for an empty structure, the passband may be varied by varying the a/b parameter. The smaller a/b is, the larger the passband becomes, and for $a/b = 1$ the passband becomes zero (easitron circuit). The relative effect of a/b on a loaded structure depends on the dielectric constant of the material and decreases with an increase in the dielectric constant. Also, generally speaking, the smaller a/b is, the smaller the transverse dimension of the structure becomes for operation at a particular frequency.

The above remarks apply generally to any dielectrically loaded structure. Figure 10 applies to a dielectric material of $\epsilon_r = 100$. It can be seen, of course, that the higher the dielectric constant, the smaller the dimensions of the structure become for operation at a particular frequency. This would be desirable at lower frequencies (X-band and lower) where the structures are large but will create *severe* demands on the required tolerances at higher frequencies. It is seen in these figures that when the material fills the space between the ladder and the plates *completely* ($d/b = 1.0$), the structure will propagate a fundamental forward wave with a slowing factor which is approximately constant through the entire passband, a characteristic which is very desirable in a traveling-wave maser. However, any minute changes in d/b will have a considerable effect on the ω-β characteristic. This stresses the severe requirements on

[6] The reader should refer to Fig. 1 for the pertinent dimensions and regions employed here.

the tolerances involved in traveling-wave masers using rutile at higher frequencies. It may also be seen in Haddad [5] that for such high dielectric constants the effect of the parameter a/b on the ω-β characteristic is slight.

2. Single-Side Loading: As mentioned earlier, single-side loading pertains to the case in which the dielectric material is placed on both sides of the ridge *either* above *or* below the ladder line (i.e., $d_2=0$). This case was also investigated for three different values of ϵ_{r2}. The results are shown in detail in Haddad [5]. The effect of the various dimensions and of the dielectric material on the ω-β characteristic is similar in this case to that of double-side loading. The only difference between the two cases is that for operation at a particular frequency the structure dimensions for single-side loading will be larger. This is to be expected, since in single-side loading the effect of the dielectric material will not be as great. Typical cases are shown in Figs. 11 and 12.

A few words are in order at this point as to the advantages and disadvantages of single- and double-side loading. From the mechanical or construction point of view, single-side loading would be desirable at high frequencies since the structure dimensions become minute, whereas double-side loading would be desirable at low frequencies where the structure dimensions are large. As to the gain in the maser amplifier, this depends on the maser material transition matrix elements and the degree of ellipticity of the RF fields in the structure. For example, if the RF fields are circularly polarized with opposite senses above and below the ladder line and the transition matrix elements are circularly polarized, then double-side loading will not result in any additional gain over that obtained with single-side loading. However, if the previous conditions are altered, then double-side loading will improve the gain. An example of this appears in Haddad and Paxman [10]. There the gain of a traveling-wave maser using ruby at X-band is discussed in detail for both single- and double-side loading.

3. Effect of Ladder-Tape Thickness: The effect of the ladder thickness on the ω-β characteristic was considered in detail and appears in Haddad [5]. It may be concluded that the ladder thickness has no effect on the lower cutoff frequency. However, if the ladder thickness is increased, the effect of the dielectric material is decreased at other frequencies in the passband. With other dimensions fixed, a thicker ladder line gives a higher upper-cutoff frequency and thus an increased bandwidth characteristic. At this value of t/q, the qualitative effects of the dielectric material and the other dimensions of the structure are essentially the same as for the previous value of t/q.

4. Effect of Ladder Pitch: For the cases considered in Haddad [5], it was shown that the pitch has a slight effect on the x vs. θ/π characteristic. However, group velocity is directly proportional to the pitch and, thus, inversely proportional to the slowing factor. The slowing factor may then be adjusted by adjusting the pitch of the structure.

5. Effect of Varying the Ratio of δ_1 to δ_2: In the previous cases, it was assumed that $\delta_1=\delta_2$; i.e., the ridge width is one half the total transverse dimension s. However, if the ridge width is made smaller, the maser material may then occupy a larger volume of the structure. This will lead to a higher filling factor and thus an improvement in the gain of the maser. x vs. θ/π is plotted for the case where the ridge width is one third the total transverse dimension s of the structure, i.e., $\delta_1=\frac{2}{3}$, $\delta_2=\frac{4}{3}$. This is done for two different values of the dielectric constant and for different dimensions of the structure. This case was investigated for single-side loading only. Some typical results are shown in Figs. 11 and 12. The qualitative effect of the dielectric material and the dimensions of the structure on the x vs. θ/π characteristic is the same in this case as in the previous ones. It can be seen from the graphs that the effect of increasing the ratio of δ_2 and δ_1 is to decrease the dimensions of the structure. This is to be expected, of course, since increasing δ_2 will extend the dielectric material farther into the high electric-field region and, thus, will increase the capacitive loading in the structure.

It should be pointed out at this point that for all the cases investigated here and in Haddad [5], the points corresponding to $\theta/\pi=0$ give approximately the cutoff frequencies for dielectrically loaded ridge waveguides, and the cases where $a/b=1$ give the cutoff frequencies for rectangular waveguides. These results then will also be useful in the design of traveling-wave masers utilizing such waveguides. Knowing the cutoff frequency is essentially all that is required for waveguide structures since this determines the dimensions. The slowing factor may be easily computed from a knowledge of the cutoff frequency and the effective dielectric constant.

Dielectrically Loaded Easitron Structure

It is well known and also can be seen from the figures that, for an empty structure, no propagation takes place when the ridge is absent, i.e., $a=b$ in Fig. 1. This is the easitron circuit, and as seen in the figures the passband is zero. It can also be seen from the figures that when the easitron circuit is loaded with a dielectric material, a finite passband results and, thus, a ridge is not required in this case. In the x vs. θ/π figures that are presented here, the figures where $a/b=1$ correspond to a dielectrically loaded easitron circuit, and it can be seen from these figures that a finite passband results for such cases. These figures correspond, however, to the cases where the dielectric material partially fills the structure and, thus, for double-side loading, corresponds to utilizing four separate slabs of dielectric material, and, for single-side loading, to two separate slabs of dielectric material. Partial loading of the structure would be desirable at lower frequencies when large single crystals of the maser material are not available. This, however, adds a complication in the construction of the maser because the two active maser material slabs must be well aligned in the structure. Due to this, and also to

the fact that at higher frequencies the slab dimensions become minute, it would be desirable to employ single slabs which completely fill the structure between the side plates, i.e., slabs of width s. This would result in a very simple structure and would be very useful in traveling-wave maser applications particularly at higher frequencies. One obvious disadvantage, of course, would be that the total transverse dimension would be smaller than that of the partially filled case. The advantages cited certainly outweigh this disadvantage by far. For this reason this case is considered here in detail.

Referring to Fig. 1, this case then corresponds to $a/b=1.0$, $\delta_1=(4l_1/s)=0$, and $\delta_2=(4l_2/s)=2$. Typical ω-β characteristics for this case are shown in Figs. 13 and 14.

Ohmic Loss in the Structure

The attenuation in nepers per meter of the structure length is given by Pierce [16] as

$$\alpha=\frac{\omega}{2Qv_g}, \tag{18}$$

where

v_g = the group velocity

and

$$Q\triangleq\frac{\omega(\text{Energy stored per tape})}{\text{Average power dissipated per tape}}.$$

An expression for Q is derived by Haddad [5].

The attenuation in dB per meter may be expressed as

$$\alpha \text{ in dB/m}=8.686\frac{\omega}{2Qv_g}. \tag{19}$$

Substituting for Q in (19) gives

$$\alpha \text{ in dB/m}=4.343(c/v_g)\frac{RF}{\eta_0}, \tag{20}$$

where

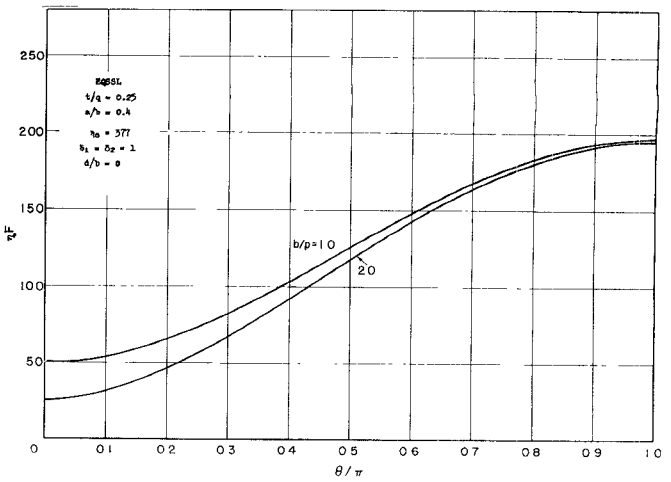

Fig. 15. $\eta_0 F$ vs. θ/π.

where

σ = the conductivity of the tape material, and
δ = the skin depth $=1/\sqrt{\pi f\mu\sigma}$.

Equation (22) may then be written in the following form:

$$R=\frac{\sqrt{\pi f\mu/\sigma}}{2q\left[\dfrac{1-\alpha}{\alpha}+\dfrac{t}{q}\right]}, \tag{23}$$

where $\alpha=q/p$.

Equation (20) may then be employed to predict the ohmic loss in the structure.

Input Impedance at the End of a Ladder Tape

One method of coupling energy into and out of the structure is through a coaxial line directly connected to the end of the tape [8]. To obtain a guideline as to the approximate magnitude of the impedance at this point[7] ($y_2=l_2$), the input impedance is defined here in terms of the power propagating on the structure, as follows:[8]

$$F=\frac{\sqrt{\epsilon_{2\text{eff}}}\,Y_{02}(\theta)\eta_0\left\{\sec^2\xi\left(1-\dfrac{\sin 2\xi}{2\xi}\right)\left(\dfrac{Y_{01}(\theta)}{\sqrt{\epsilon_{2\text{eff}}}\,Y_{02}(\theta)}\right)^2+\operatorname{cosec}^2\zeta\left(1+\dfrac{\sin 2\zeta}{2\zeta}\right)\dfrac{\delta_2}{\delta_1}\right\}}{\left\{\sec^2\xi\left(1+\dfrac{\sin 2\xi}{2\xi}\right)\left(\dfrac{Y_{01}(\theta)}{\sqrt{\epsilon_{2\text{eff}}}\,Y_{02}(\theta)}\right)+\operatorname{cosec}^2\zeta\left(1-\dfrac{\sin 2\zeta}{2\zeta}\right)\left(\dfrac{\delta_2}{\delta_1}\right)\sqrt{\epsilon_{2\text{eff}}}\right\}}, \tag{21}$$

R = the resistance per unit length of the tape, and
η_0 = the free space wave impedance = 377 ohms.

The quantity $\eta_0 F$ was plotted for several different values of the parameters [5]. Typical values appear in Fig. 15, and these values are not much different for other values of ϵ_r.

The resistance per unit length of the tape may be written as

$$R\cong\frac{1}{2\sigma[(p-q)+t]\delta}, \tag{22}$$

$$\text{Re}\,[Z_{\text{in}}]=\frac{2P}{I_{n2}(l_2)\cdot I_{n2}^*(l_2)}, \tag{24}$$

where

Z_{in} = the input impedance at the end of the tape ($y_2=l_2$),
P = the power propagating through the structure, and

[7] The reader should refer to Fig. 1 for identification of the dimensions employed here.
[8] This definition was also employed by Ash and Studd [13].

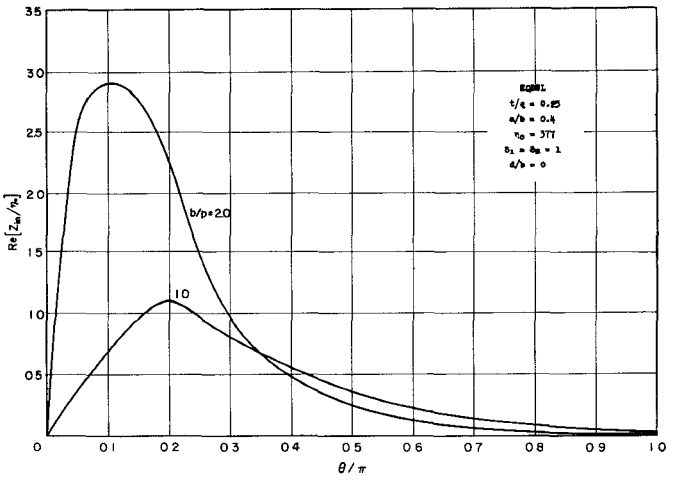

Fig. 16.

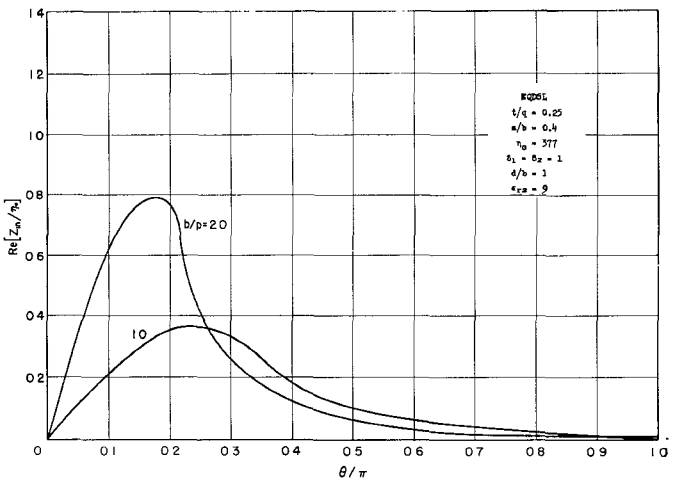

Fig. 17.

Figs. 16–17. Re $[Z_{in}]/\eta_0$ vs. θ/π.

I_n = the current int he nth tape (* indicates the complex conjugate).

A derivation of Re $[Z_{in}]$ is given in Haddad [5]. This results in

$$\frac{\text{Re}\,[Z_{in}]}{\eta_0} = \frac{\pi\delta_1}{2}\,\frac{dx/d\theta}{\sqrt{\epsilon_{2\text{eff}}}\,\eta_0 Y_{02}(\theta)} \cdot \left\{\sin^2\zeta\,\sec^2\xi\left(1+\frac{\sin 2\xi}{2\xi}\right)\frac{Y_{01}(\theta)}{\sqrt{\epsilon_{2\text{eff}}}\,Y_{02}(\theta)} + \left(1-\frac{\sin 2\zeta}{2\zeta}\right)(\delta_2/\delta_1)\sqrt{\epsilon_{2\text{eff}}}\right\}, \tag{25}$$

where

$$\eta_0 \triangleq \sqrt{\mu_0/\epsilon_0}.$$

The Re $[Z_{in}]/\eta_0$ was plotted for different values of ϵ_r and different parameters of the structure [5]. Typical cases appear in Figs. 16 and 17.

It is evident from these figures that the resistive part of the input impedance varies quite rapidly across the band and thus makes the coupling into the structure very difficult over a wide frequency range. It is worthy to note, however, that for $b/p = 1$ the impedance does not vary as rapidly, and presumably for smaller values of b/p, a smaller variation in the impedance will result and, thus, matching over a wide frequency range may be achieved in this manner.

Comparison of Theoretical and Experimental Results

The results of this analysis were employed in the design of an X-band traveling-wave maser utilizing ruby. This maser has been described in detail in Haddad and Paxman [10]. The experimental ω-β or, more specifically, the f-θ characteristics of the structure are shown in Fig. 18 where they are compared with the theoretical results.

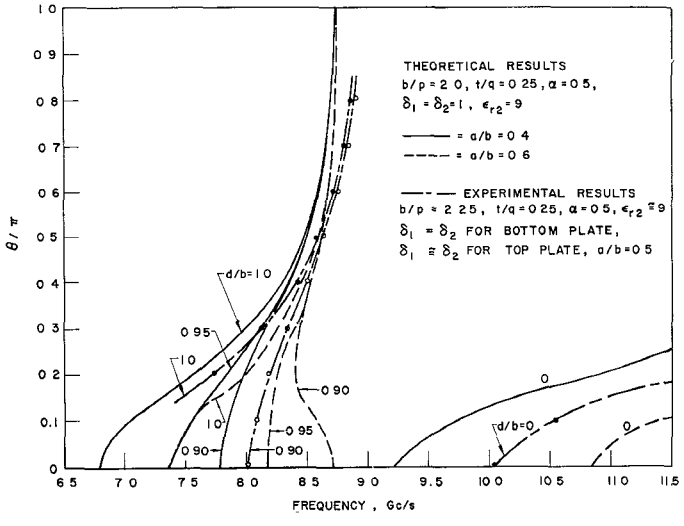

Fig. 18. Comparison of theoretical and experimental results for a ruby-loaded structure.

The test structure dimensions in inches were as follows: $s = 0.440$, $p = 0.040$, $q = 0.020$, $t = 0.005$, $b = 0.090$, $a = 0.045$, $2l_1$ for the bottom plate $= 0.220$, and $2l_1$ for the top plate $= 0.190''$. The reason for the difference in the width of the ridge of the top and bottom plates is that the ferrimagnetic isolating material was placed alongside the ruby on the top plate and, thus, enough space had to be provided for it. The dielectric constant for ruby is approximately equal to 9, and the above dimensions result in the following ratios: $b/p = 2.25$, $a/b = 0.5$, $\alpha = 0.5$, $t/q = 0.25$, $\delta_1 = \delta_2 = 1.0$ for the bottom plate but is slightly different for the top plate, and $\epsilon_{r2} = 9$. The theoretical curves are for the following ratios: $b/p = 2.0$, $\alpha = 0.5$, $t/q = 0.25$, $\delta_1 = \delta_2 = 1$ for both top and bottom plates, $\epsilon_{r2} = 9$, and for $a/b = 0.4$ and 0.6. The experimental curve would be expected to lie between the two theoretical curves for the various values of d/b because its a/b ratio lies between them and it does, except near the upper-cutoff frequency where a slight discrepancy between the experimental and theoretical results exists.

The discrepancy at the high frequency cutoff of the loaded structure may not necessarily be due to the approximations used in the analysis but may be due to the experimental measurements. For example, any minute spacing between the ladder line and the dielectric could account for the slightly higher measured upper-cutoff frequency. During the experimental measurements, it was found that the method of assembling the structure (such as how tightly the top and bottom plates are fastened together) has a large effect on the upper-cutoff frequency.

The good agreement between the theoretical and experimental results indicates the usefulness of the theoretical results in the design of dielectrically loaded ladder lines and provides confidence in the approximations employed in the analysis.

Conclusions

It may be concluded that the results presented here should be very useful in the design of ladder-line and other slow-wave structures for traveling-wave maser and other applications. The effect of a dielectric material placed at different positions in the structure has been presented, and it has been shown how the dielectric material may be placed in the structure to obtain high slowing factors. Experimental results on a ruby-loaded structure indicate good agreement with the theory. "Fold-over" modes which are undesirable in traveling-wave maser operation may be predicted and, thus, avoided. The results indicate the tolerances necessary in the construction of traveling-wave masers and how important these tolerances become at millimeter-wave frequencies when rutile is employed for the active maser material.

Acknowledgment

The author gratefully acknowledges his discussions with Prof. J. E. Rowe concerning this work. He also acknowledges the work of R. Hsieh in making calculations and plotting the graphs, of A. Pajas and A. Heath in programming the digital computer, and of R. Hsieh and J. Johnson in drawing the figures.

References

[1] R. W. Degrasse, E. O. Schulz-Dubois, and H. E. D. Scovil, "The three-level solid state traveling-wave maser," *Bell Sys. Tech. J.*, vol. 38, pp. 305–335, March 1959.
[2] R. C. Fletcher, "A broad-band interdigital circuit for use in traveling-wave type amplifiers," *Proc. IRE*, vol. 40, pp. 951–958, August 1952.
[3] A. Karp, "Traveling-wave tube experiments at millimeter wavelengths with a new, easily built, space harmonic circuit," *Proc. IRE*, vol. 43, pp. 41–46, January 1955.
[4] R. W. Degrasse, J. J. Kostelnick, and H. E. D. Scovil, "The dual channel 2390-mc traveling-wave maser," *Bell Sys. Tech. J.*, vol. 40, pp. 1117–1127, July 1961.
[5] G. I. Haddad, "Dielectrically-loaded ladder lines for traveling-wave masers and other applications," Electron Physics Lab., Elec. Engrg. Dept., The University of Michigan, Ann Arbor, Tech. Rept. 65, December 1963.
[6] S. Okwit and J. G. Smith, "Packaged electronically tunable *S*-band traveling-wave maser system," *Proc. IRE*, vol. 50, pp. 1470–1483, June 1962.
[7] W. S. C. Chang, J. Cromack, and A. E. Siegman, "Cavity and traveling-wave masers using ruby at *S*-band," *IRE WESCON Conv. Rec.*, pt. I, pp. 142–150, 1959.
[8] G. I. Haddad and J. E. Rowe, "X-band ladder-line traveling-wave maser," *IRE Trans. on Microwave Theory and Techniques*, vol. MTT-10, pp. 3–8, January 1962.
[9] K. S. Yngvesson, "A hydrogen line traveling-wave maser using chromium doped rutile," *Quantum Electronics, Proc. of the Third Internat'l Congress*, New York: Columbia University Press, 1964, pp. 899–909.
[10] G. I. Haddad and D. H. Paxman, "Traveling-wave maser experiments using ruby at *X*-band," *IEEE Trans. on Microwave Theory and Techniques*, vol. MTT-12, pp. 406–414, July 1964.
[11] P. N. Butcher, "A theoretical study of propagation along tape ladder lines," *Proc. Instn. Elect. Engns. (London)*, vol. 104, pt. B, pp. 169–176, March 1957.
[12] J. C. Walling, "Interdigital and other slow-wave structures," *J. Electronics and Control (GB)*, vol. III, pp. 239–258, September 1957.
[13] E. A. Ash and A. C. Studd, "A ladder structure for millimeter waves," *IRE Trans. on Electron Devices*, vol. ED-8, pp. 294–302, July 1961.
[14] P. N. Butcher, "The coupling impedance of tape structures," *J. Instn. Elect. Engrs (GB)*, vol. 104(B), pp. 177–187, March 1957.
[15] F. S. Chen, "The comb-type slow-wave structure for TWM applications," *Bell Sys. Tech. J.*, vol. XLIII, pp. 1035–1065, May 1964.
[16] J. R. Pierce, *Traveling-Wave Tubes*. New York. Van Nostrand, 1950, p. 95.